6-8-2012

A Shade Tolerant Panel Design for Thin Film Photovoltaics

Sourabh Dongaonkar
Purdue University - Main Campus, sourabh@purdue.edu

Muhammad A. Alam
Purdue University - Main Campus

Dongaonkar, Sourabh and Alam, Muhammad A., "A Shade Tolerant Panel Design for Thin Film Photovoltaics" (2012). *Birck and NCN Publications.* Paper 859.
http://dx.doi.org/10.1109/PVSC.2012.6318084

A Shade Tolerant Panel Design for Thin Film Photovoltaics

Sourabh Dongaonkar and Muhammad A. Alam

School of Electrical and Computer Engineering, Purdue University, West Lafayette, USA

***Abstract* — We analyze the problem of partial shading of thin film photovoltaic (TFPV) panels, using full two dimensional circuit simulations. By accounting for the panel structure and typical array configurations, we can accurately account for the effect of various shading configurations at the cell and panel level. We demonstrate the limitation of external bypass diodes in protecting shaded cells from reverse breakdown, and explore the whole range of shading scenarios and their impact on reverse stress experienced by shaded cells. Based on the analysis, we identify the key aspects of shading problem, and formulate design rules for shadow aware geometrical design of panels. Finally, we present a new radial design for a thin film PV panel, which not only improves the cell reliability under partial shading, but also enhances the array output current.**

***Index Terms* — photovoltaic systems, semiconductor device reliability, thin film devices, modeling and simulation.**

I. Introduction

The efficiencies of thin film PV technologies have improved steadily over the years, making them increasingly competitive to conventional crystalline silicon PV [1]. However, like any other technology, the variability and reliability issues will determine their ultimate commercial success [2]. An important reliability concern for PV systems is related to partial shading of panels. This problem was originally identified for crystalline silicon PV [3], and has been studied extensively since then [4]. These have been possible because of the modular structure of c-Si PV [5], which allows integrated bypass diodes inside the panel, and different wiring schemes to mitigate shading effects [6].

In case of TFPV with monolithic panel fabrication, however, the shadow effects are less well understood [7]. This is because, unlike c-Si module, series connected cells in TFPV panels are shaped like thin wide stripes. Therefore in TFPV, the shape and orientation of shadows must be taken into account carefully, to suitably estimate the effect of shadows. Also, the monolithic fabrication process of TFPV panels makes it difficult to use conventional solutions like integrated bypass diodes [8], or rewiring connections [9]. In this paper, we present a thorough analysis of shading problem in TFPV panels, using 2D spice simulations. We highlight the limitations of external bypass diodes, and explore the output loss, and reverse stress associated with different shading configurations. Based on the geometrical insights from the 2D simulations, we formulate design rules for shade tolerant TFPV panel design, and propose a new design based on radial arrangement of cells, which can alleviate shadow induced stress.

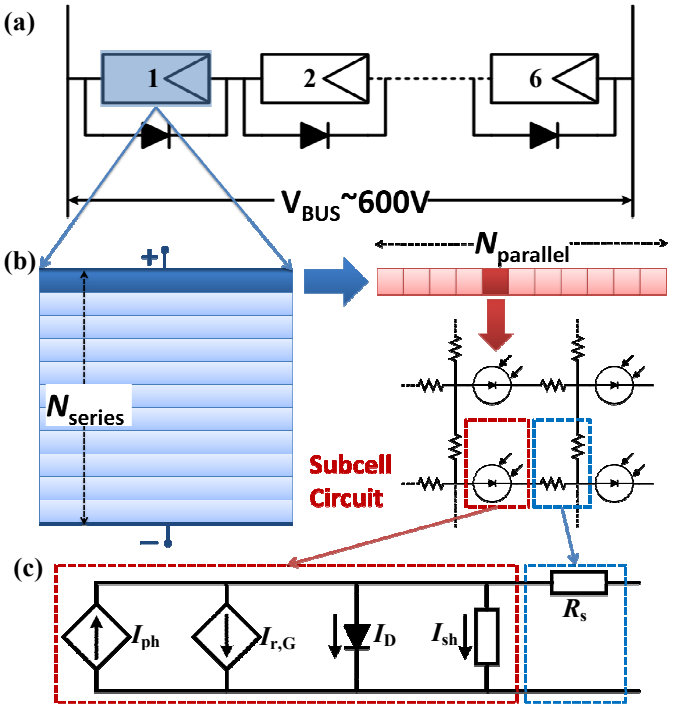

Fig. 1. (a) PV system configuration with 6 series connected panels, with external bypass diodes, connected to a system DC bus at a constant voltage of ~600V. (b) Schematic of the solar panel showing N_{series} cells, with each cell subdivided into $N_{parallel}$ subcells, connected in series and parallel to form a networked circuit representation of a TFPV panel. (c) Equivalent circuit for a-Si:H solar cells, showing various generation and leakage current components, including parasitic shunt (brown box) and contact sheet resistance (blue box) components.

II. Simulation Framework

In order to simulate the shadow effect, we need a model that can scale from the lab scale cell (~cm^2) to the panel (~m^2), and even array level.

A. SPICE Simulation framework

In order to mimic a real system closely, we simulate a string of 6 series connected panels. It is assumed that the output voltage of the panels is held constant bus voltage of 600V DC (Fig. 1a). Each panel has an external bypass diode in parallel for avoiding reverse voltages across the panels. Each panel has N_{series} rectangular cells in series (Fig. 1b shows the schematic of a typical thin film panel). Conceptually, each individual cell can be subdivided into $N_{parallel}$ 'subcells', which are connected

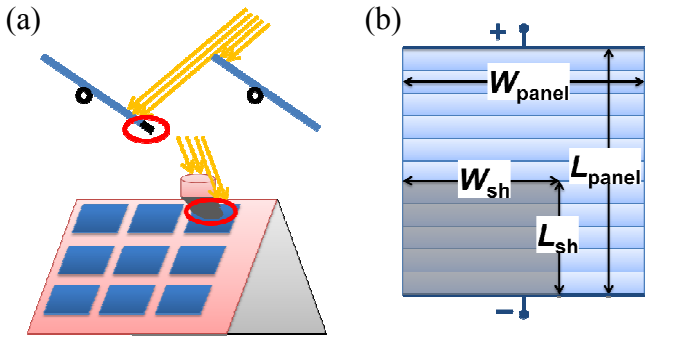

Fig. 2. (a) Schematics showing possible panel shading scenarios during normal operation, including shadow due to neighboring panels, or nearby objects. (b) Shading scenarios considered in this paper, showing rectangular shadow with dimensions W_{sh} and L_{sh} in relation to panel dimension W_{panel} and L_{panel}.

in series and parallel by the contact sheet resistance [10] (Fig. 1b). We simulate a typical a-Si:H panel (110x130 cm^2), with 110 cells in series, each 130x1 cm^2. For the sake of geometrical simplicity, the panel was assumed square (i.e. 128x128 cm^2) with 128 cells in series, instead of usual 110x130 cm^2 dimensions. The subcells themselves are represented by an equivalent circuit (Fig. 1c) developed for a-Si:H cells [11]. This ensures that correct device physics is incorporated in the circuit simulations. Depending on the technology under consideration, the equivalent circuit can modified appropriately, to account for relevant physics.

B. Modeling shading conditions

In all the simulations, it is assumed that one of 6 panels is shaded to varying degrees, due to a nearby object or neighboring panel (see schematics in Fig. 2a). The shaded region only receives diffused light which has an intensity ~20% of direct sunlight [12]. Therefore, the I_{ph} for subcells in shaded region is reduced to 20% of normal I_{ph}. Different shading conditions are explored by varying shadow length (L_{sh}) and width (W_{sh}), as shown in Fig. 2b. With these set of assumptions, we can predict the panel characteristics as a function of shading conditions, and thereby obtain quantitative estimates of shadow induced stress and power loss.

III. Role of External Bypass Diodes

We first explore the role of external bypass diode when one panel out of the string of 6 panels is partially shaded, and focus only on the panel level characteristics. In these simulations, each cell is represented by an equivalent circuit (Fig. 1c), and a panel is simply represented as a series connection of 128 such equivalent circuits in series. The shading is assumed one dimensional, assuming one cell is fully shaded at a time. The number of shaded cells is varied to explore the effect of various degrees of shading.

Fig. 3a compares the IV characteristics of shaded and unshaded panels for different degrees of shading. As the

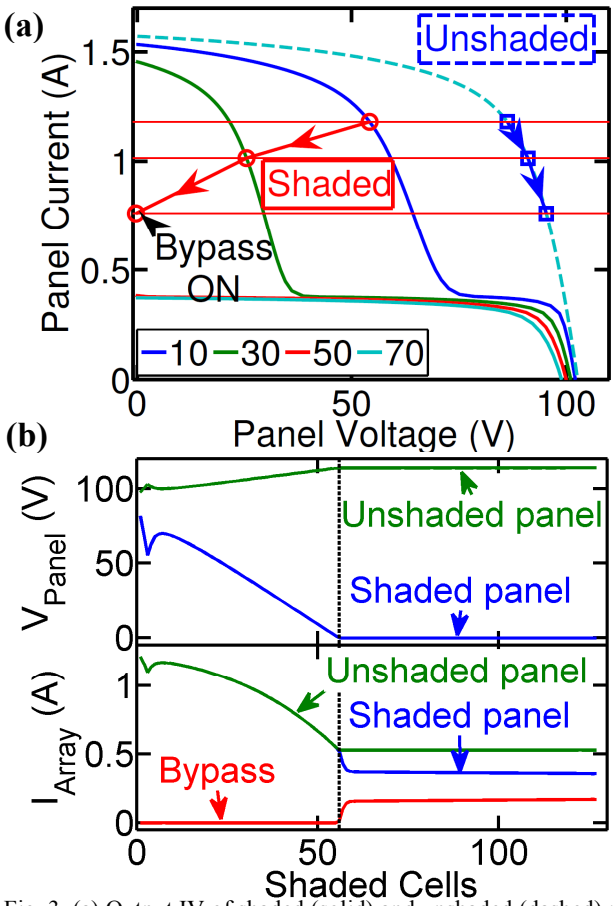

Fig. 3. (a) Output IV of shaded (solid) and unshaded (dashed) panels, with increasing shading, showing that the operating point of unshaded panels moving up (squares) and the shaded panel moving down (circles) until bypass diode turns on. (b) Panel voltages and currents as a function of number of shaded cells show that bypass diode turns on only after 50% of cells have been shaded.

current of the shaded panel drops for larger shadows, the operating voltages of shaded and unshaded panels move in opposite directions because the string voltage must be held at 600V (arrows). But, once the shading exceeds 40% of cells, the panel is pushed in reverse bias. It is only then that the bypass diode turns on and clamps the panel voltage and current. Notice that for small number of shaded cells, the bypass diode is inoperative, and cannot prevent any reverse stress across those shaded cells.

This can be seen clearly by looking at the panel voltages and currents as function of number of shaded cells. As shown in Fig. 3b, the voltage across shaded panel drops monotonically, as the number of shaded cells increases, but the bypass diode stays off. It is only when the voltage across shaded panel tries to become negative (at about N_{shaded} ~ 40% N_{series}) that the bypass diode turns on and clamps the panel voltage. This is also the case for string output current, which reduces until the bypass diode turns on and clamps it to fixed value (Fig. 3b). This means that for smaller shadows bypass diodes have no impact on the panel operation. We show next that even these

small shadows can result in extreme reverse biases on the shaded cells.

IV. Shadow Stress on Cells

In order to understand the effect of shading on individual cells, we need to consider the full 2D nature of shading patterns. In this simulation the full 2D circuit representation (as shown in Fig. 1) is used for the shaded panel; for shadows characterized by length (L_{sh}) and width (W_{sh}) shown in Fig. 2b, are varied to explore all possible rectangular shadows. Using SPICE simulations, we have verified that for rectangular shadows, the absolute position is irrelevant to its effect; the only important parameters are the number of shaded cells, and the degree of photocurrent loss in the shaded cells.

A. *Shadow size and orientation*

Fig. 4 shows the simulation results for array output current (Fig. 4a), and worst case reverse voltage across the shaded region (Fig. 4b) for all possible L_{sh} and W_{sh} values. As seen earlier, the bypass diode clamps the output only when large fractions of the panel area are shaded. The 2D simulation, however, offers insights into the importance of orientation of small shadows for TFPV panels in particular. We highlight the case of 'symmetric' edge shading (marked blue) which happens for W_{sh} < 5cm, and 'asymmetric' edge shading (marked red) which occurs for L_{sh} < 5cm.

Fig. 4a shows that these thin wide shadows do not affect array output, and the bypass diode remains off. However, when we look at the voltage distribution across shaded cells (Fig. 4b), we find that the 'asymmetric' edge shade (red) causes reverse breakdown in the shaded cells. This shows that few cells shaded along the width is the worst case scenario, causing extreme reverse bias stresses, and *which cannot be prevented by external bypass diodes*. In contrast, the 'symmetric' shade (marked blue), there is no reverse stress at all. This simulation quantitatively demonstrates the empirical observations of TFPV installers regarding 'asymmetric' and 'symmetric' shading [13].

B. *Shadow degradation*

Even if this extreme scenario is avoided, Fig. 3b shows that other shading scenarios can result in reverse stresses of 4–5 V across shaded cells. While these will not cause catastrophic device breakdown, they can result in parametric degradation over time, as reported for a-Si:H cells [14]. The integrated device-circuit simulation allows us to estimate the degradation in panel performance, in presence of such parametric stress. We have found that this degradation can be as high as 10% over the panel lifetime, which is comparable to light induced degradation in a-Si:H solar cells [15].

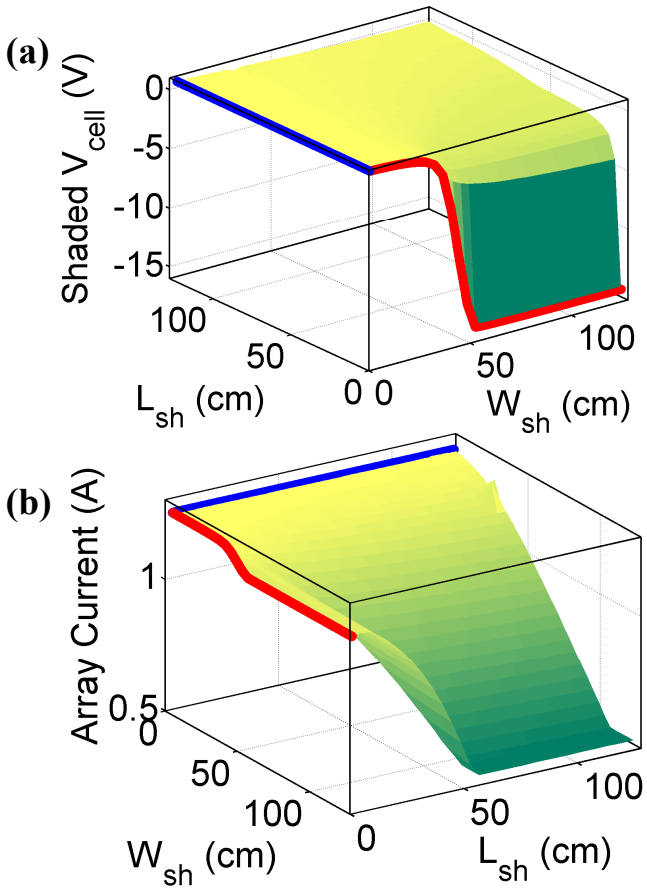

Fig. 4. (a) Array output current for different shading conditions showing that narrow shade along edges causes little output loss (blue – W_{sh}=2cm, red – L_{sh}=2cm). (b) Voltage across shaded cells for different scenarios shows that a thin edge shadow along the width (red) results in reverse breakdown of shaded cells, but edge shade along the length (blue), no reverse stress occurs. Intermediate shading (L_{sh}<L_{panel} and W_{sh}<W_{panel}) causes moderate reverse stress.

V. Geometrical Solution

A. *Geometrical design rules for TFPV panels*

The monolithic fabrication process of TFPV panels offers a unique solution to the shadow problem, because it allows arbitrary control over the shape and orientation of cells. From the analysis presented above, we can note that (1) worst case reverse stress occurs when few cells are shaded fully but rest are not (asymmetric case in Fig. 4); but (2) many cells shaded together distribute the reverse voltage amongst themselves (symmetric case in Fig. 4); and (3) panel orientation has significant impact on the effect of edge shadow. Therefore, a redesign of the shape and orientation of the cells must ensure that their arrangement is radially symmetric. However, in order to preserve the output characteristics of the panel, the area of individual cells must be identical, and number of series connected must be the same. Once such design, that can

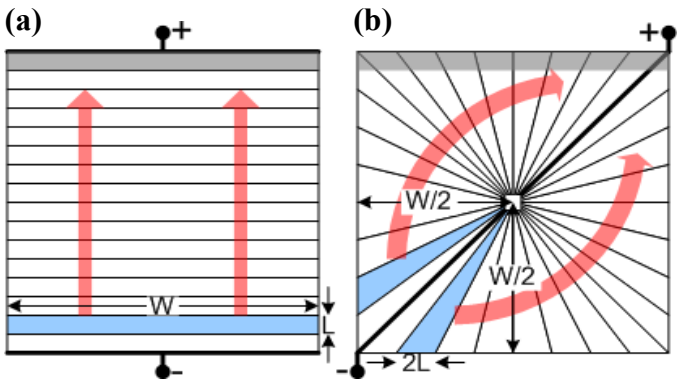

Fig. 5. (a) Typical rectangular layout of cells in TFPV panel, with terminals (bold) and current flow direction (red arrows). (b) Shadow aware design showing triangular cells arranged in a radial pattern, with terminal connection made diagonally. The edge shadow comparison shows the advantage of radial layout.

accommodate these design considerations, uses triangular cells arranged in a radial pattern (Fig. 5).

B. 'Radial' design of TFPV panel

This layout is obtained by reshaping a rectangular (WxL) cell (Fig. 5a), into two triangles with base 2L and height W/2, as highlighted in Fig. 5b. These triangles are connected in series to form two parallel strings, Note that the externally connections to the terminals now must be made diagonally (Fig. 4b). Note that for $W=N_{series}L$ the redesigned panel will have the same dimensions as the rectangular panel, with same number of cells in series. This means that the designed output of radial panel will be identical to the rectangular panel. It is straightforward to see that this design removes the problem of edge shadow causing reverse breakdown. This is because, an edge shadow shades many cells simultaneously, ensuring that the reverse voltage is distributed evenly across them.

C. Shade tolerance of radial design

We can evaluate the new design quantitatively, using the SPICE simulation framework developed for analyzing the rectangular panel earlier. In order to do this, we transform a rectangular shadow on the radial panel, into an equivalent shadow on the rectangular panel. This can be done using the same mapping used for transforming a rectangular cell to triangular, and taking the inverse transform. This will give the equivalent shadow on the rectangular panel. Once we get the number of shaded cells and their shading fraction from this transform, we can use the SPICE simulation to extract the output current loss and reverse stress for the radial design for all possible shading scenarios.

The results of the simulations comparing these designs are shown in Fig. 6, with shade dimensions depicted on x and y axes, respectively, and colors representing the output current and stress voltages. Fig. 6a compares the reverse voltage across shaded cells, for typical rectangular design vs. the radial design in Fig. 6b. Note that for all cases the radial design restricts the reverse stress to moderate values (< -6V), and

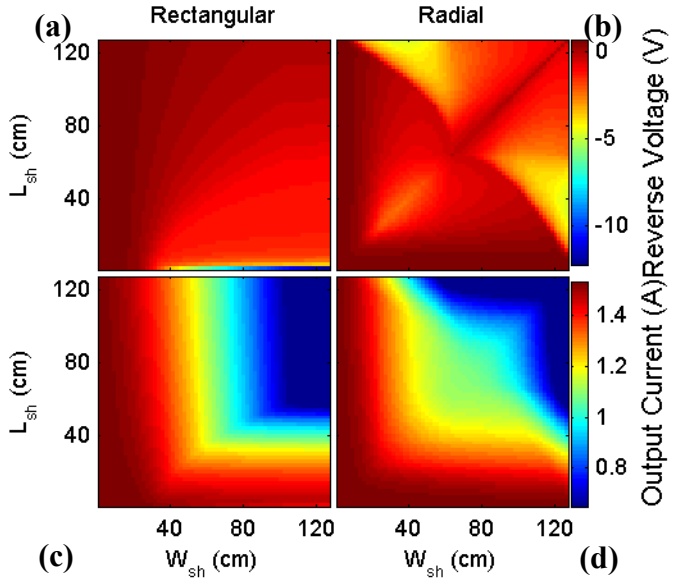

Fig. 6. 2D plots comparing shaded cell voltages (color bar in V) for normal design (a) with the radial design (b) for all possible shadows, show that the radial design restricts the reverse stress to -6V in the worst case (which happens for large shadows). Array output current (color bar in A) is also higher for radial case (d) over rectangular (c), for smaller shadows and comparable for large shadows.

avoids the worst case of reverse breakdown altogether. Moreover, the worst case reverse stress in radial design happens for large shadows, and for the more probable edge shadows, the new radial design ensure no reverse stress on shaded cells. Despite the fact that the bypass diode has remained off, the radial design manages to prevent the worst case reverse breakdown of shaded cells.

The improvement is also visible for the array output current where the radial design (Fig. 6d) ensures higher output current than the normal rectangular one (Fig. 6c), for almost all cases with $L_{shadow} < L_{panel}/2$ or $W_{shadow} < W_{panel}/2$. For large shadows the array output is comparable to the rectangular case. Thus, we see that for usual operating situations, where shadow dimensions are expected to be smaller than W_{panel} and L_{panel}, the radial design not only avoids the catastrophic breakdown of shaded cells, but also improves the array output current.

VI. Conclusion

We have explored the problem of partial shading in TFPV, for different shadow sizes. We can draw the following insights from this analysis – (a) External bypass diodes do not turn on until a large panel area is shaded. (b) Wide shadows, covering entire cell width, can cause catastrophic reverse breakdown in shaded cells, despite external bypass diodes. (c) Even when reverse breakdown is avoided, moderate reverse stresses, caused by regular shading, may lead to long term performance degradation, as demonstrated for a-Si:H cells. Based on these insights, we propose a new design for TFPV panels, in which triangular cells are laid out in a radial pattern and connected in

series. This design can avoid problem of reverse breakdown, and can alleviate shadow degradation for majority of shading scenarios.

ACKNOWLEDGEMENT

This work was supported by Semiconductor Research Corporation – Energy Research Initiative (SRC-ERI), Network for Photovoltaic Technology (NPT), grant number 204900. We would like to acknowledge the computational resources from Network for Computational Nanotechnology. We would also like to thank Dr. Michel Frei, Applied Materials, and Prof. S. Mahapatra, IIT Bombay, for support and discussions; and Dr. C. Deline, NREL for useful discussions.

REFERENCES

[1] C. A. Wolden et al., "Photovoltaic manufacturing: Present status, future prospects, and research needs," *Journal of Vacuum Science & Technology A: Vacuum, Surfaces, and Films*, vol. 29, p. 030801, 2011.

[2] R. Gaston et al., "Product reliability and thin-film photovoltaics," *Proceedings of SPIE*, vol. 7412, p. 74120N-74120N-15, 2009.

[3] R. M. Sullivan, "Shadow effects on a series-parallel array of solar cells," Greenbelt, MD, 1965.

[4] C. Deline, "Partially shaded operation of a grid-tied PV system," in *34th IEEE Photovoltaic Specialists Conference (PVSC)*, 2009, pp. 001268-001273.

[5] J. W. Bishop, "Computer simulation of the effects of electrical mismatches in photovoltaic cell interconnection circuits," *Solar Cells*, vol. 25, pp. 73-89, 1988.

[6] Y. J. Y.-J. Wang and P.-C. P. C. Hsu, "An investigation on partial shading of PV modules with different connection configurations of PV cells," *Energy*, vol. 36, no. 5, pp. 3069-3078, May 2011.

[7] A. Johansson, R. Gottschalg, and D. G. Infield, "Modelling shading on amorphous silicon single and double junction modules," in *Photovoltaic Energy Conversion, 2003. Proceedings of 3rd World Conference on*, 2004, vol. 2, pp. 1934–1937.

[8] J. H. Armstrong, S. Wiedeman, and L. M. Woods, "Monolithically integrated diodes in thin-film photovoltaic devices," U.S. Patent 669004110-Feb-2004.

[9] K. Hayashi and H. Yamagishi, "Thin film photoelectric conversion module and method of manufacturing the same," U.S. Patent 6288323Dec-2001.

[10] G. T. Koishiyev and J. R. Sites, "Impact of sheet resistance on 2-D modeling of thin-film solar cells," *Solar Energy Materials and Solar Cells*, vol. 93, no. 3, pp. 350-354, 2009.

[11] J. Merten, J. M. Asensi, C. Voz, A. V. Shah, R. Platz, and J. Andreu, "Improved equivalent circuit and analytical model for amorphous silicon solar cells and modules," *IEEE Transactions on Electron Devices*, vol. 45, no. 2, pp. 423-429, 1998.

[12] H. B. Exell, "The Intensity of Solar Radiation," 2000. [Online]. Available: http://www.homer.com.au/webdoc/science/solar/SolarRadiationIntensity.html. [Accessed: 14-Sep-2011].

[13] "KANEKA Thin Film PV Installation Manual MODULE TYPE: U-EA Type," 2011. [Online]. Available: http://www.kaneka-solar.com/download/files/manual/InstManu U-EA type.pdf. [Accessed: 06-Feb-2012].

[14] S. Dongaonkar, Y. Karthik, D. Wang, M. Frei, S. Mahapatra, and M. A. Alam, "Identification, Characterization and Implications of Shadow Degradation in Thin Film Solar Cells," in *Reliability Physics Symposium (IRPS), 2011 IEEE International*, 2011, pp. 5E.4.1 - 5E.4.5.

[15] S. Dongaonkar and M. A. Alam, "End-to-End Modeling for Variability and Reliability Analysis of Thin Film PV," in *2012 IEEE International Reliability Physics Symposium (IRPS 2012)*, 2012, pp. 4A.4.1 - 4A.4.6.